

REAL TIME PHASE CORRECTION
OF OPTICAL IMAGING SYSTEMS

BY

John W. Hardy, Julius Feinleib and
James C. Wyant

Itek Corporation
10 Maguire Road
Lexington, Mass. 02173

To be presented at the
Topical Meeting on
Optical Propagation through Turbulence
July 9-11 1974
University of Colorado,
Boulder, Colorado
Sponsored by: Optical Society of America

The possibility of compensating an optical imaging system in real time to correct for the wavefront distortion produced by propagation of the beam through a turbulent medium has been a subject of considerable recent interest. In this talk we will describe an adaptive imaging system developed at Itek that has proved the practical feasibility of real time optical phase correction, using the radiation received from a distant reference source, and show some of the results that have been obtained.

(Fig. 1) The problem that we have addressed is that of imaging a self-luminous object of small angular extent such as a planet or a double star with a telescope through turbulence that is in the near field of the objective. We require no knowledge of the structure of the object, and we are constrained to passive operation; that is; we can use only the light received from the object itself. Because the turbulence is in the near field, the distortion produced at the telescope objective is almost entirely optical phase or path length distortion. It can therefore be corrected by inserting a device such as an active mirror in the system that will insert equal and opposite path length corrections across the beam. Phase distortion is equivalent to coding the wavefront arriving at the aperture of the system; the coding consists of displacing the wavefront axially as a function of position within the pupil. If it is due to turbulence, the wavefront displacement may be changing quite rapidly.

There are two important points to note:

- 1) The wavefront displacement or coding does not in itself reduce the amount of information in the optical beam; by decoding the wavefront i.e., by putting in the appropriate displacements we can recover the original wavefront, and therefore all of the information,
- 2) The key to this code is carried in the wavefront itself. By processing the wavefront in the right way we can break the code and recover the image. This will, however, use some of the photons in the beam; the accuracy of the measurement will improve as we use more photons.

The question then arises: what is the most efficient way to use the available photons? Should we use some of them to decode the wavefront before the image is recorded, or should we just ignore the coding and use all the photons for image recording? What happens when we do nothing is shown in Fig. 2. Even a modest amount of phase distortion degrades the MTF and consequently the point spread function. The MTF may fall to zero at some frequencies due to pupil phase cancellation. With the inevitable addition of noise in the detection process, we will lose a lot of information.

In order to decode or compensate the wavefront, we need a method of determining the wavefront displacement at each location in the beam. One approach has been described by Muller and Buffington and uses the image sharpening concept. The phase or optical path length in each section of the aperture is changed sequentially and the effect on the energy density of the image or image sharpness is measured each time. The wavefront error is then corrected by maximizing the image sharpness. This approach has the disadvantage that we must use a single parameter, the sharpness function, to determine the phase errors in perhaps 100 or more independent sections of the aperture. This requires adjusting the elements serially, one at a time, necessitating very fast signal processing and a lot of light to provide the necessary dynamic range. In fact, the irradiance required from the reference source must increase with the number of wavefront correction elements for a single-image sharpening system. The image-sharpening approach is therefore not suitable for use with faint objects or with large apertures.

The wavefront measuring and correcting system developed at Itek is shown diagrammatically in Fig. 3. It operates in the aperture of the optical system where the wavefront distortion is not dispersed. The wavefront distortion is a function of time and of position within the aperture; it may therefore be easily separated out for measurement. For simplicity, operation is shown with a wavefront sinusoidally deformed in one dimension; the system is capable of operating with two-dimensional random wavefront distortion.

The essential steps in the Itek system are:

- (1) To place a path-length correction device in the incoming beam;

- (2) To shear the wavefront by a shear distance S which can be varied to suit the operating conditions, thereby obtaining a shearing interferogram of the wavefront;
- (3) To measure the phase of this interferogram simultaneously at a number of locations in the aperture, the spacing of these measuring locations being determined by the coherence length of the wavefront disturbance. These phase measurements reveal the slope of the wavefront at each location;
- (4) To compute from these measured slope values, the actual profile of the wavefront across the aperture, using a parallel data processor;
- (5) To apply feedback voltages corresponding to the inverse of the measured wavefront to the path length correction device, thereby nulling the wavefront distortion

The important features of this system are:

The system is inherently wide-band, because the parameter being measured and corrected is optical path length. This is compatible with the effects of atmospheric turbulence because air has a low dispersion. This feature allows the use of a broad spectral band for measurement, providing efficient operation with white-light reference sources.

The optical path length difference is measured separately and simultaneously over each section of the aperture. The area of each section would be determined by the expected size of the turbulence cells. There are two important consequences

- (1) the limiting magnitude of the entire system is determined only by the area of each section of the aperture and by its integration time; the overall size of the aperture and the number of sections may be increased without loss of efficiency.
- (2) Because of parallel operation, the response time of the system is virtually independent of the number of correction channels.

The system does not require the use of a point reference source. The effect of a reference source of finite angular extent is to reduce the contrast of the fringes, and therefore to reduce the signal to noise ratio, but there are no other effects.

The system can be optimized in real time to meet fluctuating conditions, by varying the shear distance for example to accommodate different amounts of path length distortion.

Wavefront Measurement

The basic principles of the lateral shearing interferometer are shown in Fig. 4. Two diffraction gratings having slightly different line spacings are placed near the focal plane of the telescope. For any given wavelength of light, this produces two diffracted cones of rays at two slightly different angles. The diffraction angle is chosen large enough to keep the zero-order undiffracted rays separate. The amount of shear is determined by the angular difference between the two diffracted beams. In practice, the two grating frequencies are produced holographically on a single plate.

A second diffraction grating having a line spacing midway between the two frequencies on the initial grating is then introduced into the beam.

The field lens then produces two white images of the telescope entrance pupil, enabling operation in white light. By translating the two-frequency grating laterally, the phase at each location is ac modulated at a frequency determined by the grating frequency and the velocity of translation. This process makes possible the use of a parallel electro-optical detector array coupled to parallel electronic signal processing channels. The need for time sharing between detector outputs is therefore eliminated and the entire interference pattern can be detected and processed within times in the order of 1 millisecond.

A lateral shearing interferometer enables the relative phase shift at an array of points in the sheared image plane to be measured. To reconstruct the actual shape of the measured wavefront, it is necessary to obtain at least two sets of phase values by shearing in two directions (usually, but

not necessarily, orthogonal). The resulting phase data must then be reduced; for an equal sampling density in the two orthogonal directions, the number of phase measurements approaches twice the number of wavefront points determined. The wavefront is therefore overdetermined and a smoothing technique can be used to reduce random errors.

In the Itek system, a parallel analog computer is used to perform this function. Operation of the computer is illustrated in Fig. 5.

The wavefront phase shifts measured by the shearing interferometer are shown by the horizontal and vertical arrows. The points at which the phase errors are evaluated are shown as round dots.

It can be seen that any point such as N is connected to the outside world only through the four phase shift vectors a, b, c and d, which are algebraically added to the phase shifts existing at the points A, B, C, and D. The phase shift value at N is therefore

$$N = (A + B + C + D + a - b - c + d) / 4$$

The required function may be realized by using a conduction matrix with each grid point representing a computed phase point on the wavefront. A current proportional to the algebraic sum of the four adjacent phase measurements (a - b - c + d) is injected into each grid point, and the resulting voltage at each grid point then represents the average phase at the corresponding point on the wavefront.

Using this approach, it is possible to process any practical number of inputs in a time of less than 1 millisecond.

Wavefront Correction

In a practical real-time wavefront correction system designed for an astronomical telescope, the wavefront correction is implemented at a much reduced image of the telescope entrance pupil. The wavefront correction device may therefore be of small diameter (about 1 inch) and capable of high frequency response.

For this application, Itek has developed a new generation of wavefront correction devices, using the piezoelectric deformation of a monolithic block.

Phase Corrector Device

Optical Wavefront correction devices must be stable to a small fraction of an optical wavelength, requiring an extremely precise, rigid construction and a stable reference plane from which the mirror displacements can be made, while minimizing the effects of thermal distortions. Such mirrors, using individual mechanical or piezoelectric actuators, have been difficult to achieve and the large masses required for stable configurations have made for slow devices. In addition, point forces applied to a free standing mirror substrate generally cause coupled bending and deflections at other points on the mirror. Thus, complicated calculations must be performed in order to achieve a given mirror figure from a fixed set of actuators. Our approach at solving this problem was to use a single piece of piezoelectric with many addressable electrodes attached to achieve a monolithic mirror configuration.

The monolithic piezoelectric phase corrector is shown in Fig. 6. The device consists of a disk of ceramic piezoelectric material (PZT) on the top surface of which is mounted an array of independently addressed electrodes, with a common electrode on the lower surface. The disk is so proportioned-that local deformations due to the piezoelectric effect take place at the top surface only, with negligible overall deformation of the disk. A thin wafer of glass, which is cemented to the top surface, is polished and aluminized to form the optically reflecting element.

In this configuration, the electrode structure underneath the mirror is well resolved and there appears to be little coupling from one electrode element to another. Subsequent computer calculations of the behavior of a ceramic block with inhomogenous electric fields applied at various points on the surface showed that for thick devices, the displacement of the top piezoelectric surface follows the voltage distribution precisely. There is a negligible change in piezoelectric sensitivity with spatial frequency. This simple construction, called a monolithic piezoelectric mirror (MPM), therefore proved to have many desirable operating characteristics: it is a single piece of material so that is thermally stable, the piezoelectric displacements do not depend on a precise reference substrate for their relative displacements, the device is rugged and is easily polished to a figure of better than 1/20 wave across the entire surface. The device used in the prototype system consisted of 21 addressable electrodes in a

1 1/2 in. diameter device of about 1/2 in. thick. The piezoelectric response of the device is better than a kilohertz and no undesirable effects of hysteresis were found. It is clear that this monolithic construction allows the device to be scaled up to many hundreds of elements easily, without sacrificing compactness and ruggedness.

Feasibility Model

A feasibility model real time wavefront correction system based on the principles described above has been built and tested in the laboratory. Photographs of the equipment are shown in Figs. 7 and 8.

The system used a 21 element MPM wavefront corrector with a correction range of about 2 wavelengths at 0.633 nm. The AC shearing interferometer employed for wavefront measurement provided 32 simultaneous phase difference measurements across the aperture at a 2 KHz rate; in other words; the measuring system provided 64,000 separate phase measurements per second.

Test Results

The test results we show here were obtained with a He-Ne reference source; the wavefront distortion was generated in the laboratory by a figured glass plate and also by thermally induced turbulence.

Fig. 3 shows the effect of the system on the laser point spread function with varying amounts of static wavefront distortion. Measurements of the encircled power are shown in each case. The results of these tests are summarized in Fig. 10, which indicates that the experimental system is capable of reducing the RMS wavefront error by a factor of better than 5 within the range tested.

Dynamic response of the system is also shown in Fig. 10. These are actually loop-closing transients showing the time required to correct the indicated distortion, starting with the loop open.

We conclude this presentation by showing a short 16 mm movie of the laser point spread function being corrected in real time in the presence of dynamic wavefront distortion generated by a moving glass disk, and by thermal turbulence.

The work described in this paper was supported in part by the Defense Advanced Research Projects Agency and the contract was administered and monitored by Rome Air Development Center.

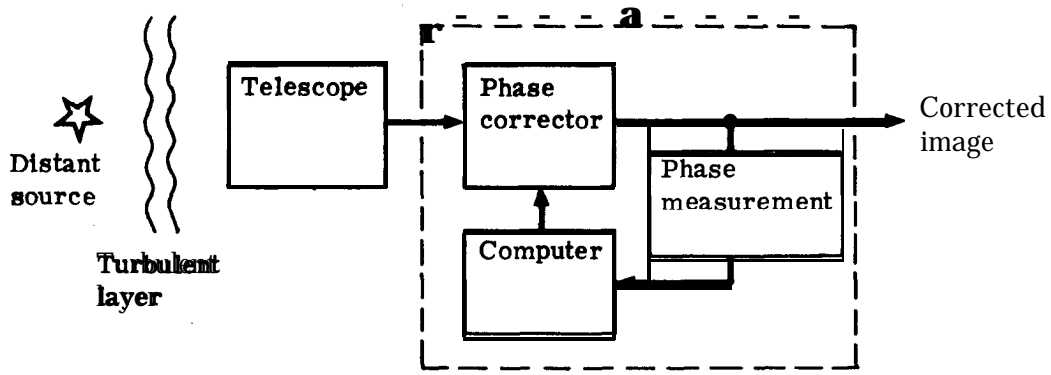


Fig. 1 - Real-time optical phase correction system

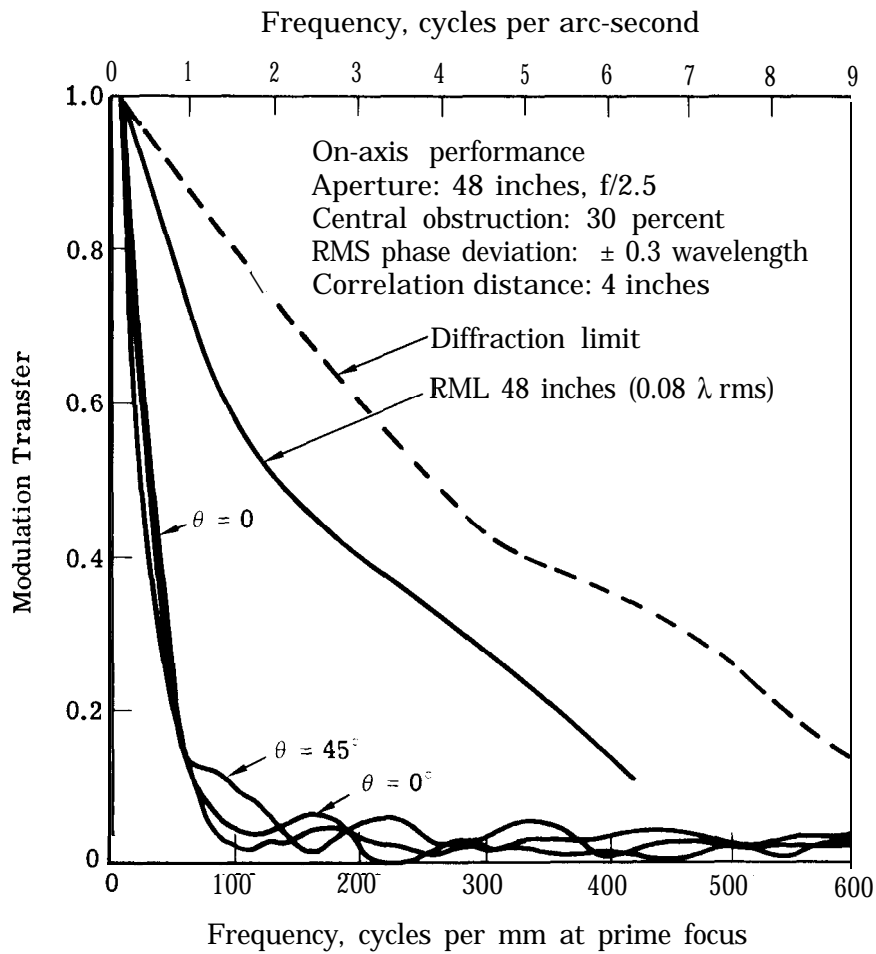


Fig. 2 - MTF curves of a 48-inch telescope

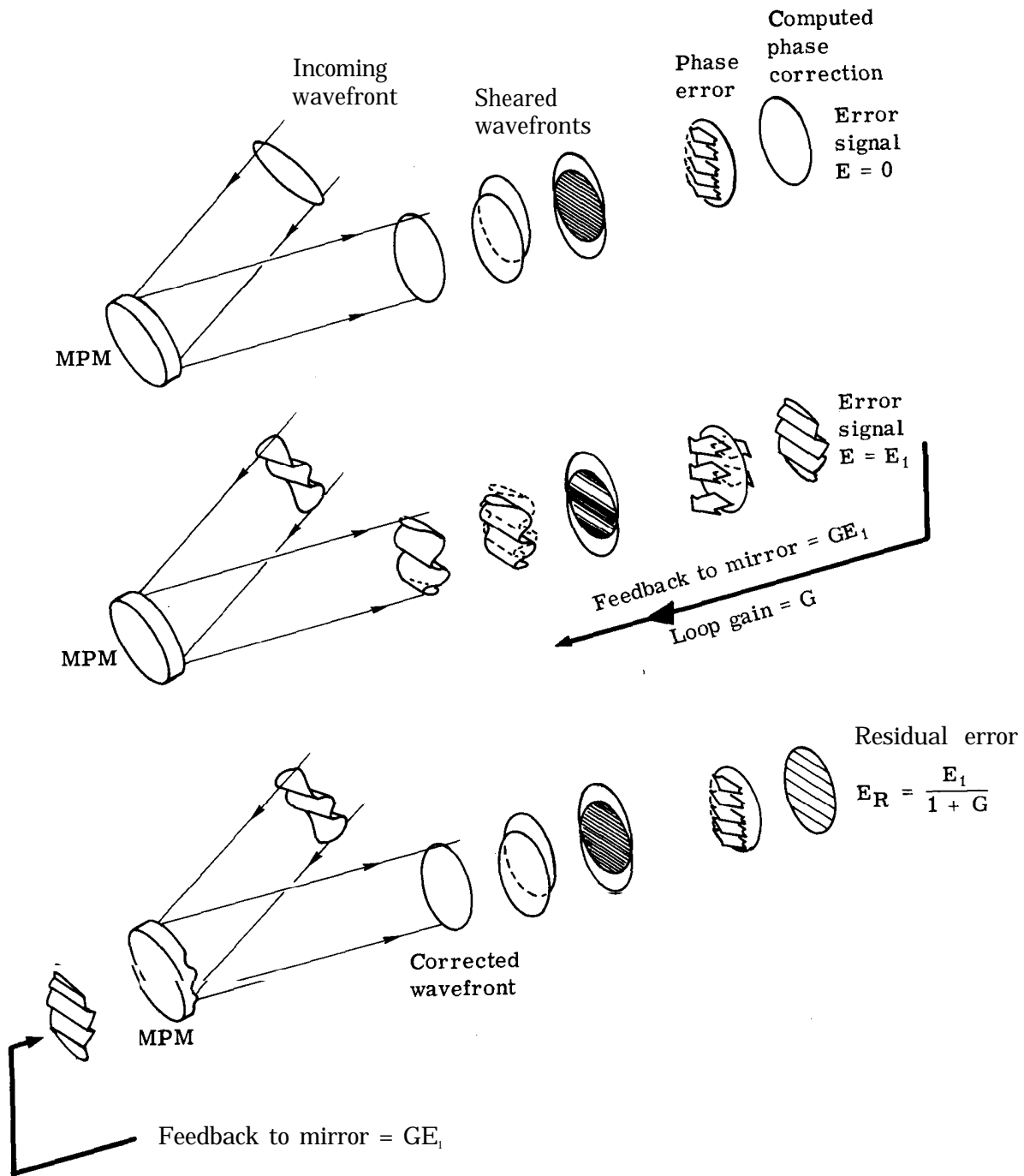


Fig. 3 - Itek wavefront measuring and correction system

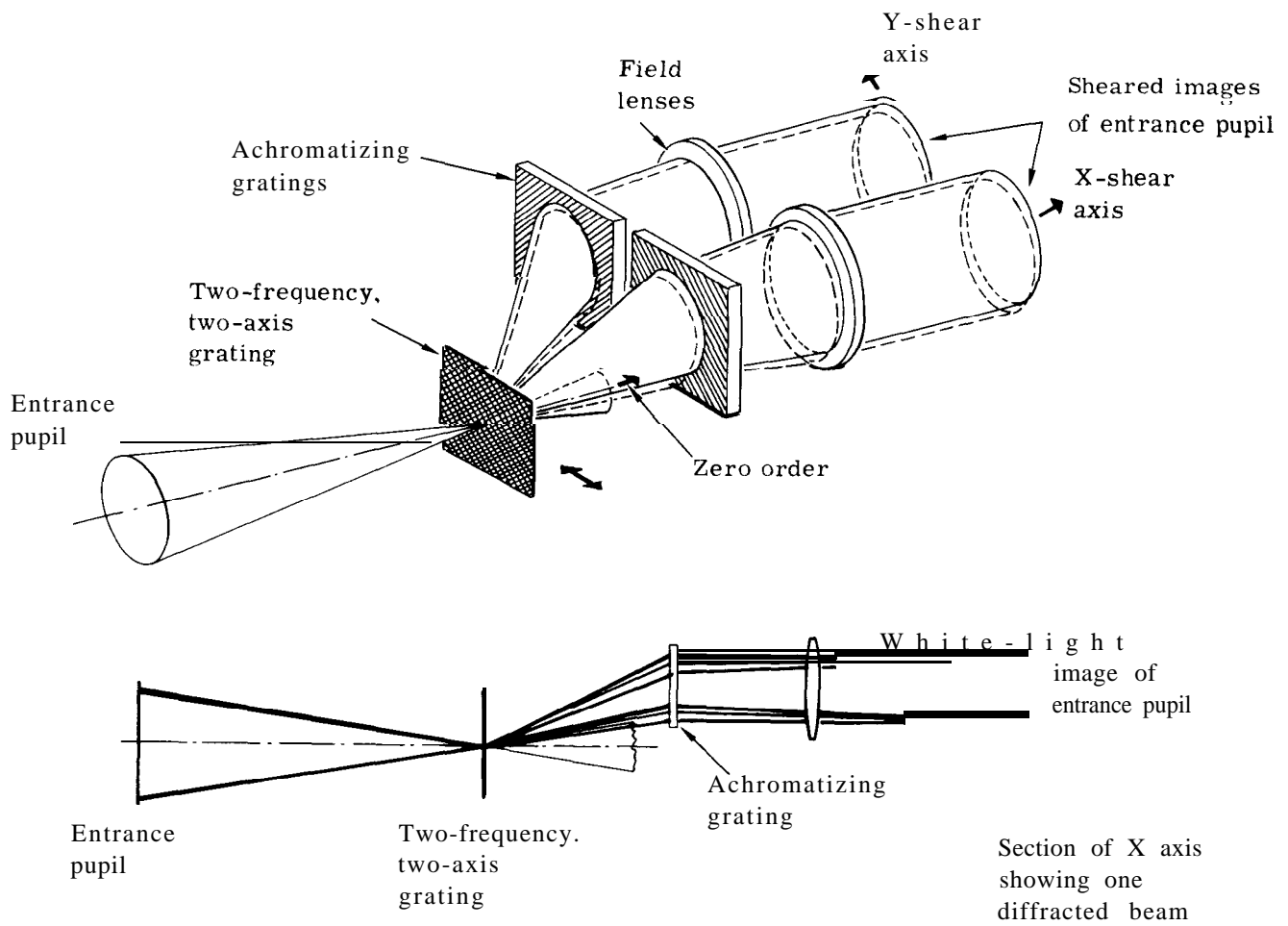
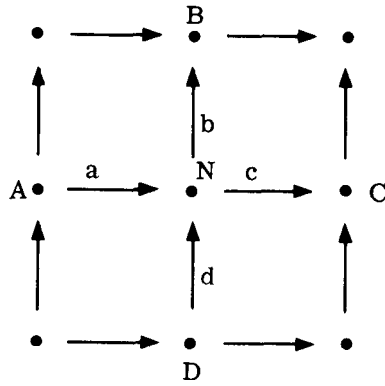
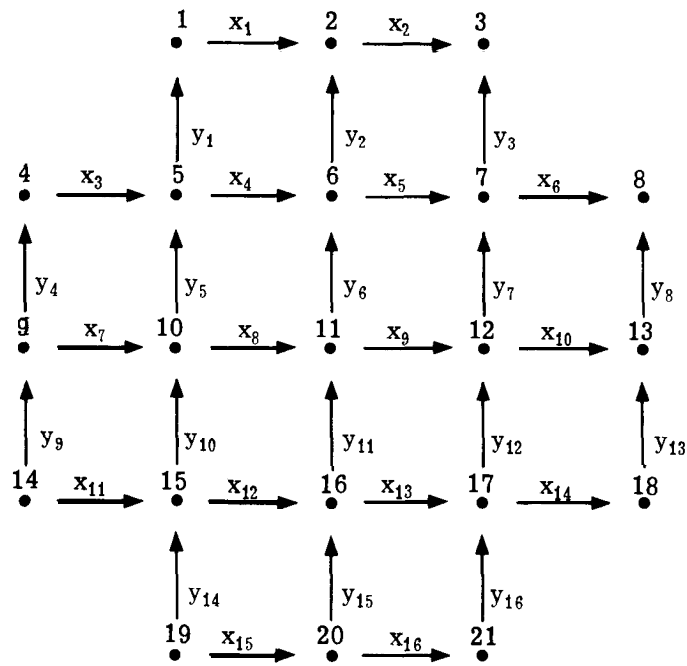


Fig. 4 - Principle of ac lateral shearing interferometer



$$N = (1/4)(A + B + C + D + a - b - c + d)$$

(a) Phase determination at one point



(b) Complete matrix

Fig. 5 - Computation of phase element values

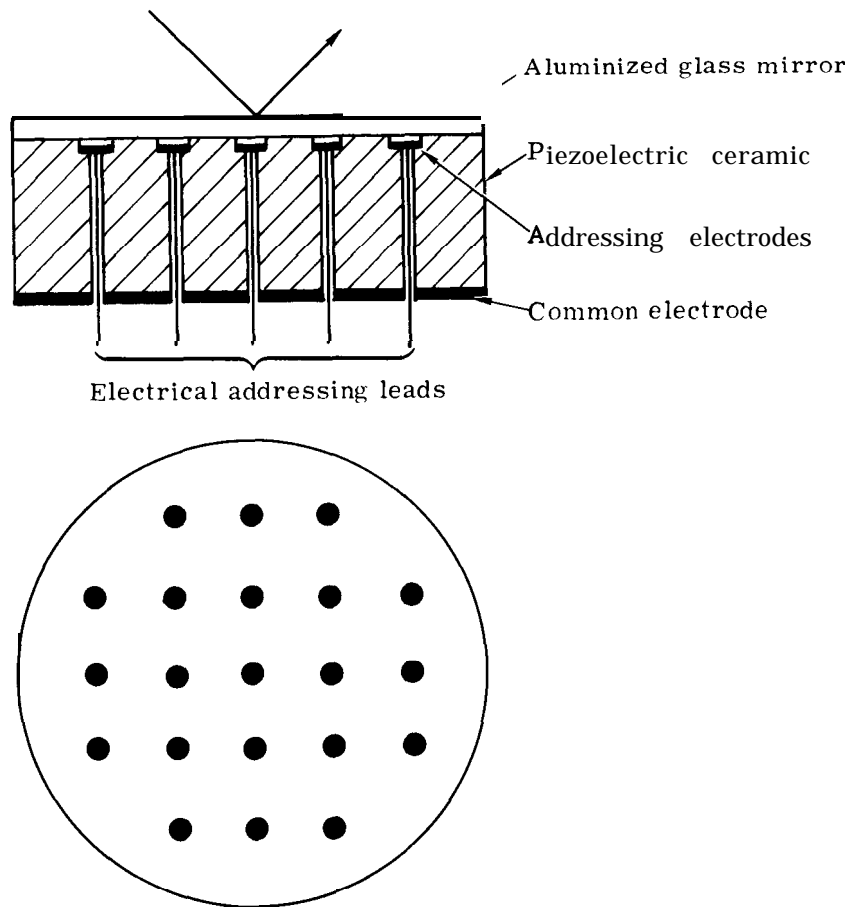
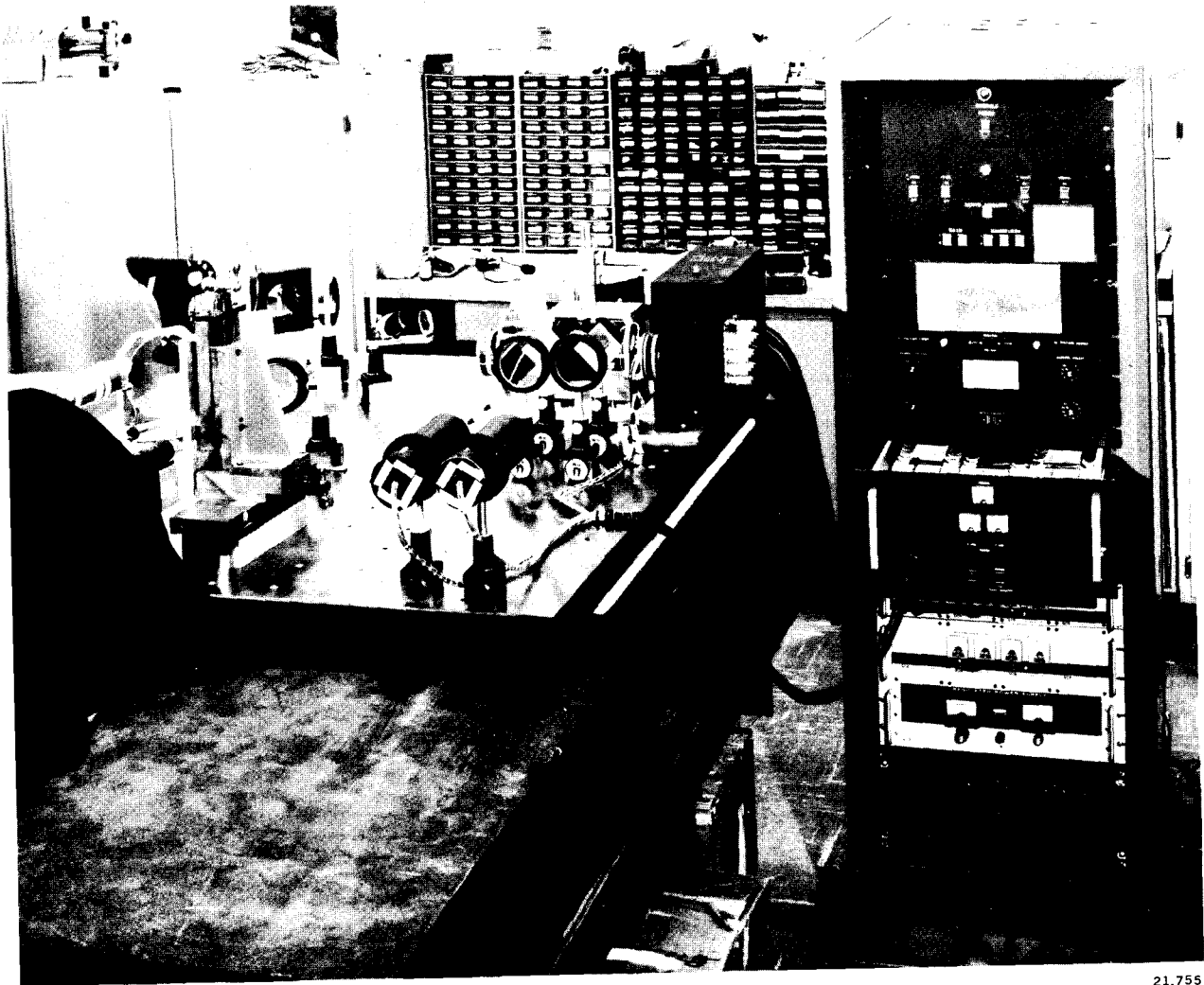
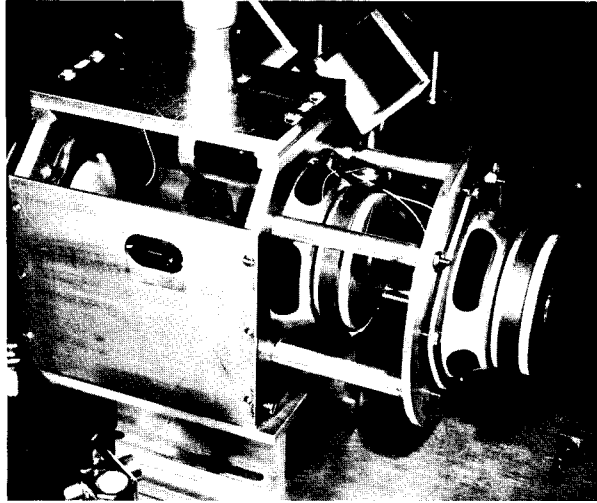


Fig. 6 - Monolithic piezoelectric mirror



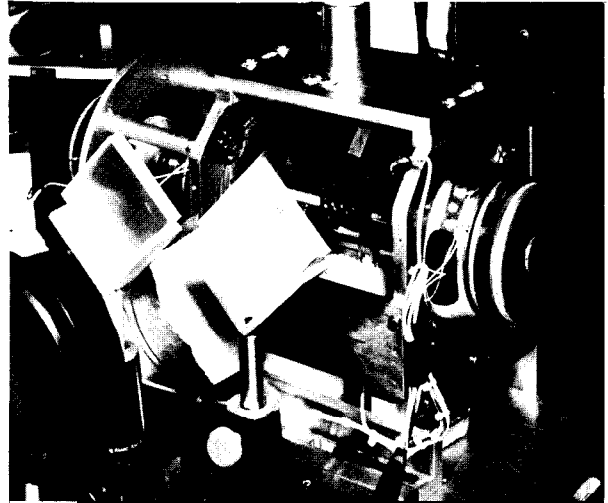
21,755

Photograph of laboratory feasibility model



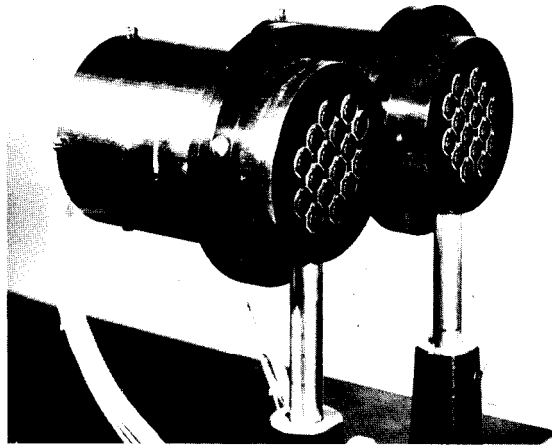
21,757

Front



21,753

Back



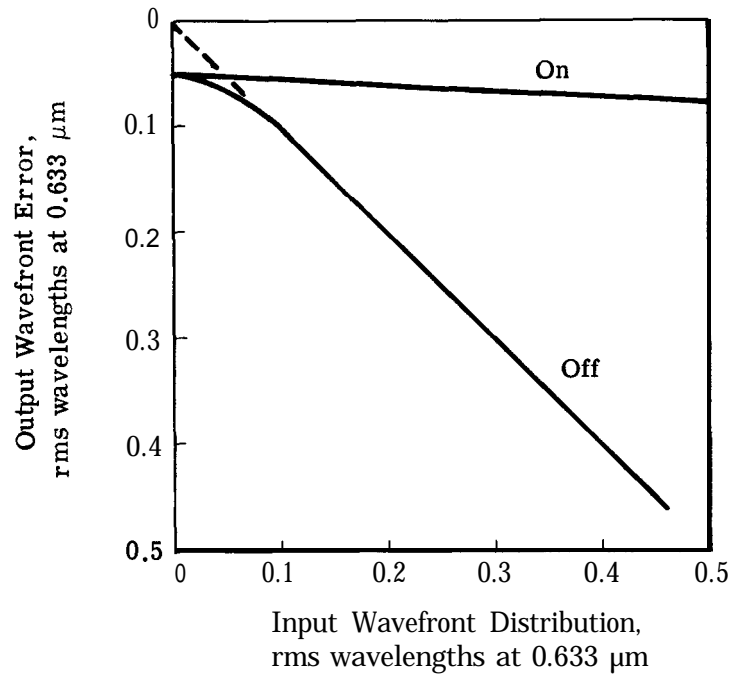
21,756

Detector arrays

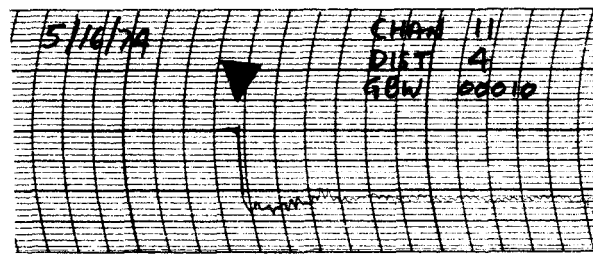
Photograph of shearing interferometer

Input Wavefront Distortion		Wavefront Correction System Off		Wavefront Correction System On		
Peak, waves	RMS, waves	Point Spread Function	Encircled Power in Central Disk, percent	Point Spread Function	Encircled Power in Central Disk, percent	RMS Distortion, waves
None	None				90	0.05
0.75	0.24		26		81	0.07
1.5	0.51		39		77	0.076

Fig. 9 - Correction of laser point spread functions (encircled power indicated)



(a) Wavefront distortion correction



→ Time
200 msec per division

(b) Response time, loop closed with 1.5 waves peak input distortion

Fig. 10 - Performance of real-time wavefront correction system